

Coherent Bunching of Anyons and their Dissociation in Interference Experiments

Bikash Ghosh¹, Maria Labendik¹, Vladimir Umansky¹,

Moty Heiblum^{1,#}, and David F. Mross²

¹ Braun Center for Submicron Research & Department of Condensed Matter Physics

² Department of Condensed Matter Physics, Weizmann Institute of Science, Israel

Corresponding author

Aharonov-Bohm (AB) interference in fractional quantum Hall states generally reveals the fractional charge e^* of their elementary quasiparticles. Indeed, flux periods of $\Delta\Phi=(e/e^*)\Phi_0$ were observed in interference of ‘particle-like’ fractional states. Here, we report interference measurements of ‘particle-hole conjugated’ states at filling factors $\nu=2/3$, $3/5$, and $4/7$, revealing the unexpected periodicities, $\Delta\Phi=\nu^{-1}\Phi_0$. Moreover, the measured shot noise *Fano factor* (F) of partitioned quasiparticles in the interferometer’s quantum point contacts (QPCs) was $F=\nu$ and not the expected $F=e^*/e$. These combined observations indicate that fractional quasiparticles tunnel in the QPCs and interfere as coherently bunched pairs, triples, and quadruplets, respectively. Charging a small metallic gate in the center of the two-path interferometer forms an antidot (or a dot) and introduces local quasiparticles, leading, unexpectedly, to a dissociation of the bunched quasiparticles, thus restoring the flux periodicity set by the elementary quasiparticle charge. The surprising observations of *bunching* and *dissociation*, unsupported by current theory, suggest similar effects in particle-like states at lower temperatures.

Interference measurements of quantum particles offer detailed insights into their single-particle dynamics and collective behavior. Such measurements are particularly valuable for emergent exotic particles that form due to strong interactions between electrons in two dimensions. These particles carry a fractional charge, obey anyonic statistics, and produce specific macroscopic signatures such as fractionally quantized conductance and thermal quantum Hall effects.

The properties of individual fractional quasiparticles (QPs) exhibit striking deviations from those of weakly interacting electrons. Experiments were designed to measure the scattering phase

shifts and quantum coherence times ¹; test entanglement between a pair of quantum particles ²; and probe the quasiparticle charge ³⁻⁵. The braiding phase was measured via interference experiments using Fabry–Perot interferometers ⁶⁻¹⁷ or Mach–Zehnder interferometers ¹⁸⁻²⁰, with distinct fingerprints of the charge and the statistics of interfering quasiparticles. Recently, *time-braiding* was utilized to measure the anyonic statistical phase via cross-correlation of partitioned quasiparticles ²¹⁻²³.

In any fractional quantum Hall (FQH) interferometer, the interference loop involves partitioning in two QPCs (serving as beam-splitters) and ballistic propagation along edge channels surrounding the bulk. The QPCs partition the incoming beam into discrete fractional charge quanta, determined by the bulk filling ν_b , leading to shot noise characterized by a *Fano factor*, F ³⁻⁵. In contrast, the gapless edge (or interface) channels impose no constraints, and the interference signal is independent of their choice ²⁴. As the partitioned charge is responsible for the interference, the Aharonov-Bohm (AB) flux periodicity must follow the simple rule, $\Delta\Phi = \Phi_0/F$. We note that in previous measurements performed with the particle states $\nu=2/5$ and $\nu=3/7$, the Fano factor did not match the value expected for the elementary quasiparticle charge (e^*/e) allowed by the FQH bulk. Instead, it followed the filling, namely: $F \cong 2e^*/e$ with $e^*=e/5$ and $F \cong 3e^*/e$ with $e^*=e/7$, respectively, at a temperature of $\sim 9\text{mK}$ ²⁵. A similar behavior was also observed in ‘particle-hole conjugated’ states ^{26,27}. This behavior could arise, for example, if coherent QPs, formed by pairs or triplets of the elementary QPs, tunnel at the QPC. Specifically, the Fano factors imply a QP charge, $e_\Phi = \nu e$, which corresponds to the insertion of one flux quantum, sometimes referred to as a *Laughlin QP*, distinct from *elementary QPs* with charge e^* (the two coincide for Laughlin states such as $\nu=1/3$). Alternatively, neutral modes (topological or ‘edge-reconstructed’) could yield additional partition noise due to stochastic equilibration processes, thus increasing the Fano factor to a value larger than e^*/e ²⁸. However, the obtained flux periodicity in interference measurements reflects coherent quasiparticle behavior and can thus distinguish between the two scenarios.

Our measurements were performed with a chiral (optical-like) Mach-Zehnder Interferometer (OMZI) ^{24,29,30} (Fig. 1). Its flexible design, based on co-propagating *interface modes* is free of

Coulomb interactions and provides access to different fractional fillings. The OMZI already demonstrated interfering flux periodicities as large as $7\Phi_0$ at bulk filling $\nu_b=3/7$ [24](#). In this interferometer architecture, two charged external gates define the interfering interface modes: one *depletes* carriers to filling ν_d , while the other *accumulates* carriers to filling ν_a . The edge conductances of the two interface modes are set by the fillings differences $\nu_b-\nu_d$ and $\nu_a-\nu_b$. Two QPCs, labeled ‘QPC1’ and ‘QPC2’ in [Fig. 1](#), partition the co-propagating interface modes to form the interference loop. The chirality of the interface modes prohibits back reflection, and consequently, the OMZI displays a pristine AB interference pattern, known as ‘pajama’ [24](#). To obtain phase slips in the AB interference, quasiparticles are introduced in the bulk of the interferometer by charging a small top gate (TG), thus forming an isolated *antidot* (or a dot) in the center of the interferometer ([Fig. 1](#)) [24](#).

Previous OMZI studies of three particle-like bulk fillings $\nu_b=1/3$, $2/5$, and $3/7$, found AB interference with magnetic flux periodicities $\Delta\Phi\cong(e/e^*)\Phi_0$, set by the elementary quasiparticle charges, $e^*\cong e/3$, $e/5$, and $e/7$, respectively, at an electrons’ temperature 15-20mK [24](#). Here, we present AB interference and noise measurements at *particle-hole conjugated* bulk fillings $\nu_b=2/3$, $3/5$, and $4/7$.

We first measured the shot noise of a single QPC, obtaining the Fano factor, $F=\nu_b=e_\Phi/e$, instead of the common $F\cong e^*/e$ ([Fig. 2](#)). These measurements agree with earlier studies at a similar temperature range [26,27](#). Moreover, and surprisingly, the observed magnetic flux periodicity $\Delta\Phi$ was not the ordinary integer multiple of Φ_0 ; it was non-integer at all three fillings and agreed with the measured Fano factor; namely, $\Delta\Phi \cong \frac{1}{F} \Phi_0 = \frac{e}{e_\Phi} \Phi_0$ ([Fig. 3](#)).

The expected periodicity in the ‘modulation gate’ voltage, V_{MG} , can be derived as follows. The flux periodicity revealed by the modulation gate should also be $\Delta\Phi=\frac{e}{e_\Phi}\Phi_0$. The gate repels the charge $\Delta Q=C\times\Delta V_{MG}$ with the capacitance C assumed to be independent of ν_b , leading to a filling-

factor independent periodicity $\Delta V_{\text{MG}} (e_{\Phi}/e) B = \Phi_0 \Pi$, with $\Pi = ne/C$. We find nearly identical values of $\Delta V_{\text{MG}}(2/3, 3/5, 4/7) = (11.7\text{mV}, 10.3\text{mV}, \text{and } 9.5\text{mV})$.

Since the noise Fano factor (Fig. 2) and the AB periodicity (Fig. 3) go hand-by-hand, we conclude that coherent QPs with charge e_{Φ} are tunneling across both QPCs and interfering. At the measured fillings $\nu_b = 2/3, 3/5$, and $4/7$, the tunneling Laughlin QPs in the QPCs are equivalent to pairs, triplets, or quadruplets of elementary QPs. This observation defies theoretical expectations based on bulk QP gaps and scaling dimensions at the edge, which are expected to be the smallest elementary QPs. For $\nu_b = 2/3$, we measured the periodicity $\Delta\Phi = (3/2)\Phi_0$ in the configurations $(\nu_d, \nu_b, \nu_a) = (0, 2/3, 4/3), (0, 2/3, 1)$, and $(1/3, 2/3, 1)$. Notably, the latter configuration is the particle-hole conjugate of $(0, 1/3, 2/3)$, where $\Delta\Phi = 3\Phi_0$ was observed²⁴. For $\nu_b = 3/5$ and $4/7$, the depleted and accumulated fillings were the integers 0 and 1, respectively.

Introducing localized QPs by charging the gate with $V_{\text{TG}} \cong -100\text{mV}$ (forming an antidot) or with $V_{\text{TG}} = +50\text{mV}$ (dot) led to another surprising effect. The magnetic field periodicity amounted to $\Delta\Phi \cong (e/e^*)\Phi_0$ at all three tested fillings, similar to the observed AB periodicity of Jain particle-like states²⁴ [Fig. 4 (a, c, e)]. This behavior indicates the *dissociation* of Laughlin QPs into elementary ones. For some parameter choices, the dissociation was incomplete, and a weaker FFT component of the bunched periodicity $\Delta\Phi \cong (e/e_{\Phi})\Phi_0$ remained [Fig. 4 (b, d, f)]. See also Supp. Sections S4 and S7.

For the ‘modulation gate’ voltage periodicity of the dissociated QPs, assuming the same modulation gate capacitance and replacing the previous Fano factor $F = e_{\Phi}/e$ by $F = e^*/e$, leads to $\Delta V_{\text{MG}}(e^*/e) B = \Phi_0 \Pi$, with $\Pi = ne/C$. While the periodicities ΔV_{MG} were quite similar in the bunched cases, and in agreement with expectations, they deviated significantly in the dissociated cases, namely, $\Delta V_{\text{MG}}(2/3, 3/5, 4/7) = (21.7\text{mV}, 17.4\text{mV}, 15.5\text{mV})$. While this is not understood, we may speculate that the ‘gate-mode capacitance’ changes with a different filling.

Due to these surprising observations, we repeated the experiment with a second OMZI device featuring slightly higher transmission of every QPC and a smaller top gate radius, $\sim 0.35\mu\text{m}$. The measurements confirmed the bunching and dissociation at fillings $\nu_b=2/3$ and $\nu_b=3/5$ (See Supplementary [S6](#) and [S7](#)). The filling $\nu_b=4/7$ was not tested.

Due to the higher visibility at $\nu_b=3/5$ in the second device, we tested the dissociation of the bunched QPs in this state. For a sequence of positive top gate voltages in the range, $V_{\text{TG}} \cong 0\text{--}70\text{mV}$, the flux periodicity changed continuously as the QPs dissociated with the varying V_{TG} ([Fig. 5](#)). Starting with the *bunched periodicity* $\Delta\Phi=(5/3)\Phi_0$ and ending at a dissociated periodicity at $V_{\text{TG}}=60\text{mV}$ with $\Delta\Phi=5\Phi_0$, while a weaker *bunched periodicity* still remained. For $V_{\text{TG}}>60\text{mV}$, dissociation stopped, and only the bunched periodicity $\Delta\Phi=(5/3)\Phi_0$ is visible, suggesting the absence of localized QPs in the dot.

Tunneling across each QPC is influenced by multiple factors. First, the bulk filling at the QPC determines which QPs can tunnel, e.g., the elementary QPs with charge e^* or Laughlin QPs with charge $e_\Phi=e\nu_b$. Second, the tunneling process is expected to be influenced by the bulk energy gaps of different QPs and renormalized by the gapless edge states. However, the observed shot noise and interference do not depend significantly on the specific edge state, and the origin of e_Φ tunneling here and in earlier experiments^{[24](#) [26,27](#)} remains unknown. The present experiments, conducted at very low temperatures and in a relatively weak magnetic field, provide vital insights for addressing this question: the increased Fano factor, $F = e_\Phi/e$ arises due to a coherent process, indicating a quantum mechanical origin. Moreover, the dramatic change of the AB interference pattern upon charging an isolated antidot (or dot), thus introducing localized QPs, indicates that quantum statistical effects impact what types of QPs interfere. Control over the interfering quasiparticles will be critical in the search for non-Abelian statistics since the Laughlin quasiparticles are Abelian even in non-Abelian quantum Hall states such as the Moore-Read Pfaffian ^{[31](#)}.

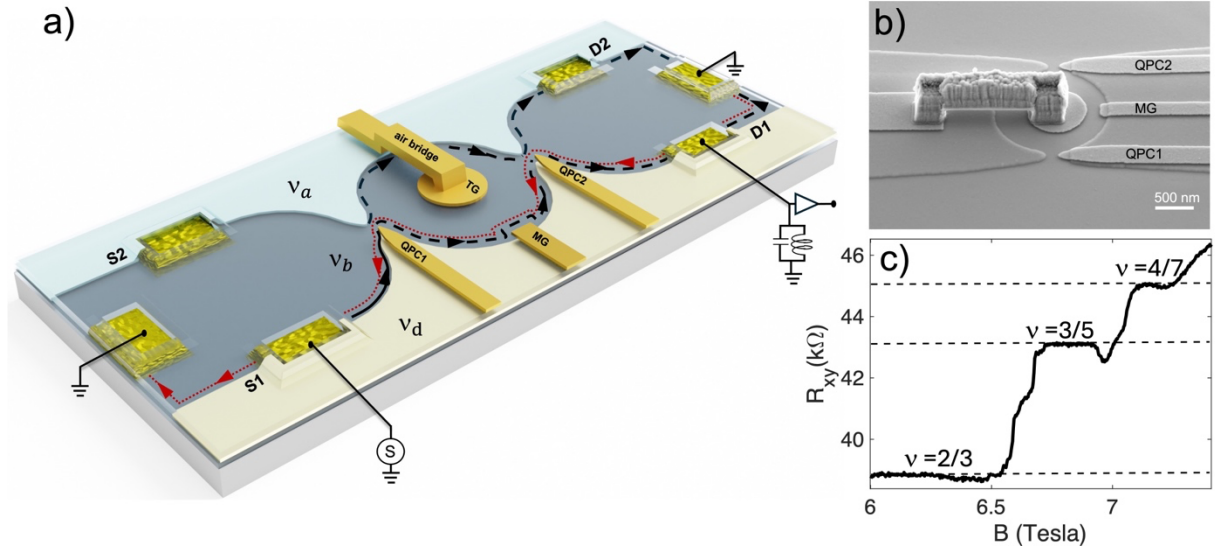


Figure 1: Device structure of an optical Mach-Zehnder interferometer (OMZI).

(a) Schematic representation of the OMZI. It is structured with three regions, each tuned to a different filling factor. The central region (the bulk, dark gray) is tuned by the magnetic field B to filling ν_b . It is flanked by two boundary regions, each tuned to different filling using wide metallic gates. The upper gate (light blue) is positively charged, thus *accumulating* the 2DEG charge, leading to a higher filling, $\nu_a > \nu_b$. The lower gate (light yellow) is negatively charged and depletes the 2DEG to a lower filling, $\nu_b > \nu_d$. This combination results in two co-propagating interface charge modes, $\nu_a - \nu_b$ and $\nu_b - \nu_d$, respectively. This design prevents backscattering of the interface modes and is free of Coulomb interactions. Current is sourced from contact S1 (or S2) at 766 KHz. It partitions at QPC1 into two forward-propagating chiral edge modes partitioned further by QPC2. Black dashed lines indicate the downstream charge edge modes, while red dotted line stands for the upstream neutral edge modes. The transmitted current is collected by drains D1 and D2 and is amplified by a cold amplifier. A small metallic ‘top gate’ (TG) is deposited at the center of the interferometer bulk, inducing an antidot (or a dot) that can introduce localized quasiparticles. **(b)** A scanning electron micrograph image of the heart of the interferometer.

(c) The transverse Hall resistance as a function of the magnetic field showing quantized plateaus at the fractional fillings under study.

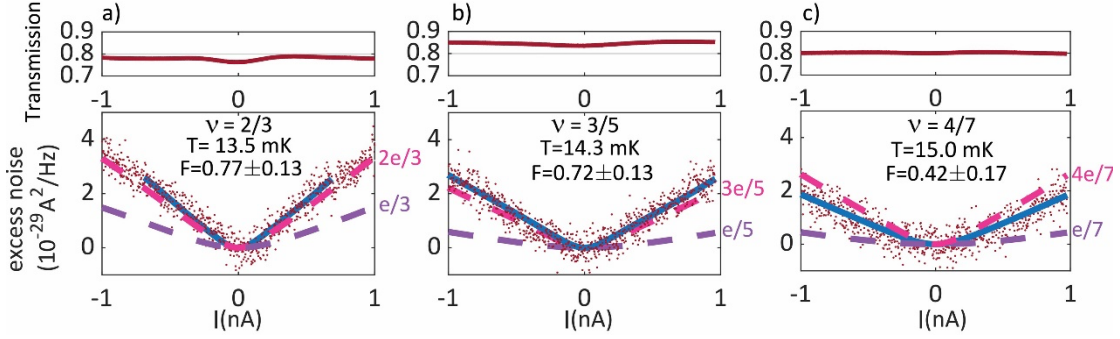


Figure 2. Shot noise measured in a single QPC. Noise was measured for three particle-hole conjugated states with bulk fillings: **(a)** $\nu=2/3$, **(b)** $\nu=3/5$, **(c)** $\nu=4/7$. Top panels: Nonlinear transmissions of the QPC. Bottom panels: Excess noise as a function of the sourced current. The blue lines represent the fitted curves and the Fano factor, F . The dashed pink lines indicate $F=\nu_b$, and the dashed purple lines are $F=e^*/e$.

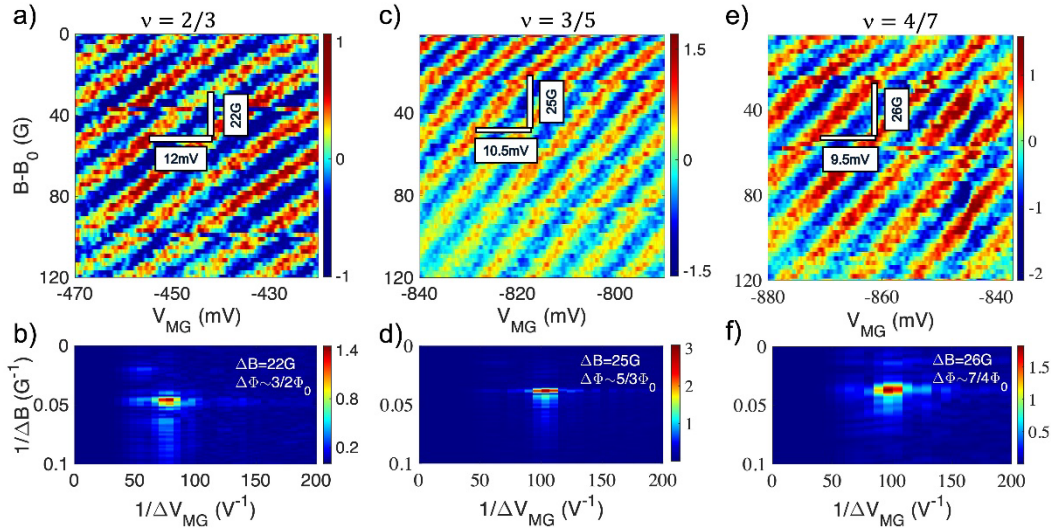


Figure 3. Evidence of coherent bunching of anyons in particle-hole conjugated states. Aharonov-Bohm (AB) interference (pajamas) of the three states plotted as a function of magnetic field B and modulation gate voltage V_{MG} . Each of the two QPCs is tuned to transmission, $T_1=T_2=0.8$, while the antidot's (or dot's) top gate (TG) is not charged. The pajamas and the corresponding 2D Fast Fourier Transforms (FFTs) relate to the states: **(a, b)** $\nu_b=2/3$, **(c, d)** $\nu_b=3/5$, and **(e, f)** $\nu_b=4/7$. The fractional flux periodicities are $\Delta\Phi \cong \nu_b \Phi_0$ in all three cases.

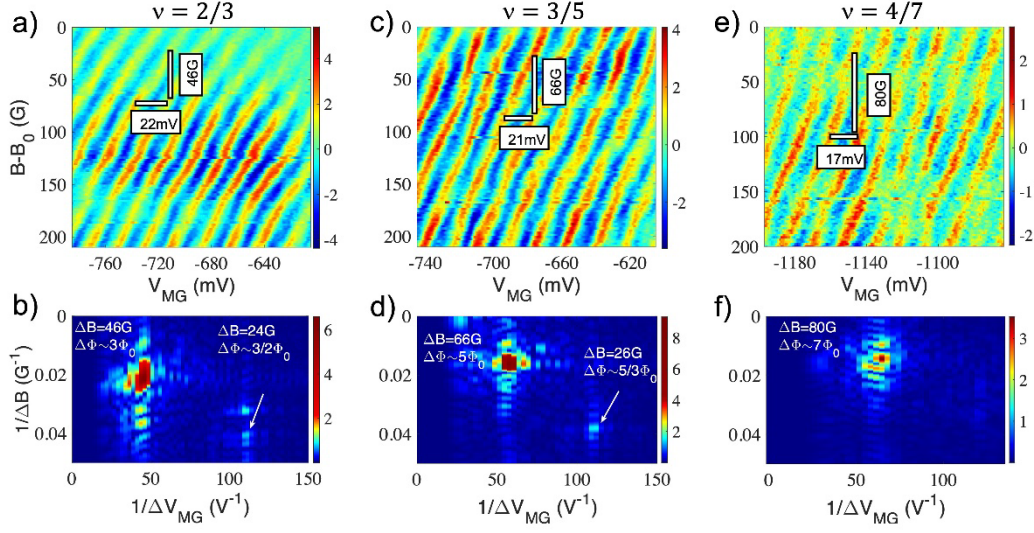


Figure 4. Evidence of coherent dissociation of bunched anyons in particle-hole conjugated states. Activating the top gate with $V_{TG}=-(100-120)$ mV forms an antidot that harbors an isolated quasiparticle. An apparent dissociation of the bunched anyons takes place. Figures **(a)**, **(c)**, and **(e)** show typical AB pajamas in the B - V_{MG} plane. The two QPCs transmissions ($T_1=T_2=0.8$) are unaffected by V_{TG} . The FFTs in figures **(b)**, **(d)**, and **(f)** reflect the flux periodicities: $\Delta\Phi \cong (e/e^*)\Phi_0$, corresponding to the interference of the elementary fractional charges, $e/3$, $e/5$, and $e/7$. A weak higher harmonic due to residual bunching is also observable in $\nu_b=2/3$ and $\nu_b=3/5$, however, at filling $\nu_b=4/7$ the ‘bunched periodicity’ is absent.

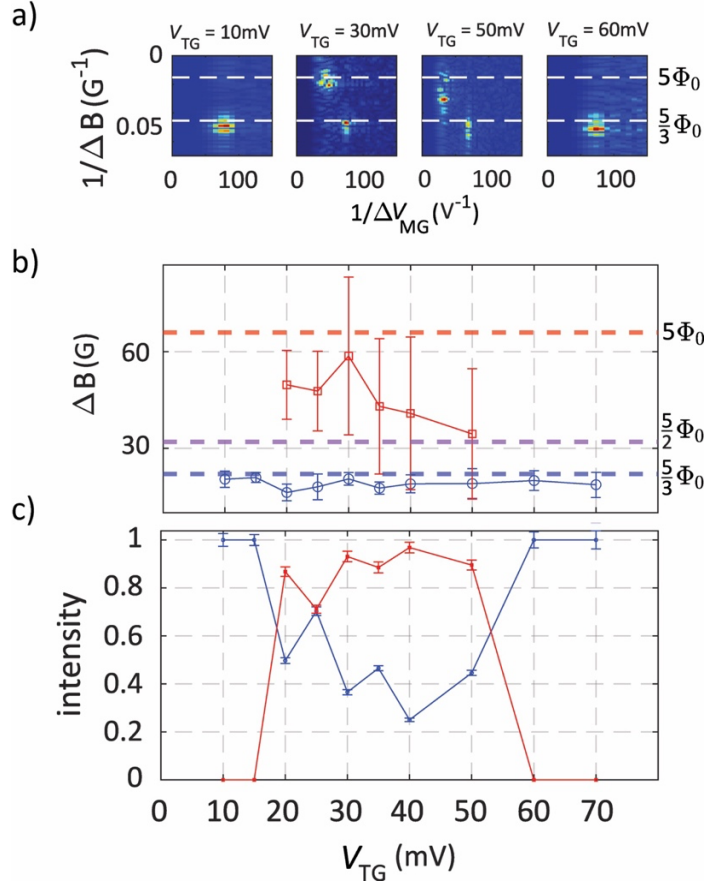


Figure 5. Evolution of the dissociated anyons with charging the top gate at $\nu_b=3/5$. The top gate (TG) was charged incrementally in steps of $\Delta V_{TG}=5$ mV in the range $V_{TG}=0-70$ mV, and the AB pajamas in the B - V_{MG} plane were recorded at each step. **(a)** The ΔB peak positions in the 2D FFT as a function of V_{TG} . When the TG is charged below $V_{TG}=20$ mV or above $V_{TG}=50$ mV, the QPs remain bunched, with flux periodicity $\Delta\Phi=(5/3)\Phi_0$. **(a, b)** An apparent dissociation (red) of the bunched anyons (blue) takes place in the range $V_{TG}=(20-50)$ mV, showing partial $\Delta\Phi=(5/2)\Phi_0$ and full dissociation $\Delta\Phi=5\Phi_0$. A residual, weaker, bunched peak remains. The error bars indicate the width of each peak, determined from a Gaussian fit. **(c)** Relative weights of the bunched (blue) and dissociated (red) FFT peaks as a function of V_{TG} .

References

- 1 Schuster, R. *et al.* Phase measurement in a quantum dot via a double-slit interference experiment. *Nature* **385**, 417-420 (1997).
<https://doi.org/10.1038/385417a0>
- 2 Neder, I. *et al.* Interference between two indistinguishable electrons from independent sources. *Nature* **448**, 333-337 (2007). <https://doi.org/10.1038/nature05955>
- 3 dePicciotto, R. *et al.* Direct observation of a fractional charge. *Nature* **389**, 162-164 (1997). <https://doi.org/10.1038/38241>
- 4 Saminadayar, L., Glattli, D. C., Jin, Y. & Etienne, B. Observation of the $e/3$ fractionally charged Laughlin quasiparticle. *Physical Review Letters* **79**, 2526-2529 (1997).
[https://doi.org/DOI 10.1103/PhysRevLett.79.2526](https://doi.org/DOI%2010.1103/PhysRevLett.79.2526)
- 5 Simmons, J. A. *et al.* Resistance fluctuations in the integral-quantum-Hall-effect and fractional-quantum-Hall-effect regimes. *Physical Review B* **44**, 12933-12944 (1991).
[https://doi.org/DOI 10.1103/PhysRevB.44.12933](https://doi.org/DOI%2010.1103/PhysRevB.44.12933)
- 6 Zhang, Y. M. *et al.* Distinct signatures for Coulomb blockade and Aharonov-Bohm interference in electronic Fabry-Perot interferometers. *Physical Review B* **79**, 241304 (2009). [https://doi.org/ARTN 24130410.1103/PhysRevB.79.241304](https://doi.org/ARTN%2024130410.1103/PhysRevB.79.241304)
- 7 Ofek, N. *et al.* Role of interactions in an electronic Fabry-Perot interferometer operating in the quantum Hall effect regime. *Proceedings of the National Academy of Sciences* **107**, 5276-5281 (2010). <https://doi.org/10.1073/pnas.0912624107>
- 8 Nakamura, J., Liang, S., Gardner, G. C. & Manfra, M. J. Direct observation of anyonic braiding statistics. *Nature Physics* **16**, 931-936 (2020). <https://doi.org/10.1038/s41567-020-1019-1>
- 9 Ronen, Y. *et al.* Aharonov-Bohm effect in graphene-based Fabry-Pérot quantum Hall interferometers. *Nat Nanotechnol* **16**, 563-569 (2021). <https://doi.org/10.1038/s41565-021-00861-z>
- 10 Kim, J. *et al.* Aharonov-Bohm interference and statistical phase-jump evolution in fractional quantum Hall states in bilayer graphene. *Nature Nanotechnology* (2024).
<https://doi.org/10.1038/s41565-024-01751-w>
- 11 Nakamura, J. *et al.* Aharonov-Bohm interference of fractional quantum Hall edge modes. *Nature Physics* **15**, 563-569 (2019). <https://doi.org/10.1038/s41567-019-0441-8>
- 12 Déprez, C. *et al.* A tunable Fabry-Pérot quantum Hall interferometer in graphene. *Nat Nanotechnol* **16**, 555-562 (2021). <https://doi.org/10.1038/s41565-021-00847-x>
- 13 Samuelson, N. L. *et al.* Anyonic statistics and slow quasiparticle dynamics in a graphene fractional quantum Hall interferometer. arXiv:2403.19628 (2024).
<<https://ui.adsabs.harvard.edu/abs/2024arXiv240319628S>>.
- 14 Werkmeister, T. *et al.* Anyon braiding and telegraph noise in a graphene interferometer. arXiv:2403.18983 (2024). <<https://ui.adsabs.harvard.edu/abs/2024arXiv240318983W>>.
- 15 Chamon, C. D. C., Freed, D. E., Kivelson, S. A., Sondhi, S. L. & Wen, X. G. Two point-contact interferometer for quantum Hall systems. *Physical Review B* **55**, 2331-2343 (1997). [https://doi.org/DOI 10.1103/PhysRevB.55.2331](https://doi.org/DOI%2010.1103/PhysRevB.55.2331)

- 16 Willett, R. L. *et al.* Interference Measurements of Non-Abelian $\nu=4/5$ & Abelian $\nu=2/5$ Quasiparticle Braiding. *Physical Review X* **13**, 011028 (2023).
<https://doi.org/10.1103/PhysRevX.13.011028>
- 17 Yang, W. *et al.* Evidence for correlated electron pairs and triplets in quantum Hall interferometers. *Nature Communications* **15**, 10064 (2024).
<https://doi.org/10.1038/s41467-024-54211-3>
- 18 Ji, Y. *et al.* An electronic Mach-Zehnder interferometer. *Nature* **422**, 415-418 (2003).
<https://doi.org/10.1038/nature01503>
- 19 Neder, I., Heiblum, M., Levinson, Y., Mahalu, D. & Umansky, V. Unexpected behavior in a two-path electron interferometer. *Physical Review Letters* **96**, 016804 (2006).
<https://doi.org/10.1103/PhysRevLett.96.016804>
- 20 Kundu, H. K., Biswas, S., Ofek, N., Umansky, V. & Heiblum, M. Anyonic interference and braiding phase in a Mach-Zehnder interferometer. *Nature Physics* **19**, 515-521 (2023).
<https://doi.org/10.1038/s41567-022-01899-z>
- 21 Lee, J.-Y. M. *et al.* Partitioning of diluted anyons reveals their braiding statistics. *Nature* **617**, 277-281 (2023). <https://doi.org/10.1038/s41586-023-05883-2>
- 22 Glidic, P. *et al.* Cross-Correlation Investigation of Anyon Statistics in the $\nu=1/3$ and $2/5$ Fractional Quantum Hall States. *Physical Review X* **13**, 011030 (2023).
<https://doi.org/10.1103/PhysRevX.13.011030>
- 23 Ruelle, M. *et al.* Comparing Fractional Quantum Hall Laughlin and Jain Topological Orders with the Anyon Collider. *Physical Review X* **13**, 011031 (2023).
<https://doi.org/10.1103/PhysRevX.13.011031>
- 24 Ghosh, B. *et al.* Anyonic Braiding in a Chiral Mach-Zehnder Interferometer. arXiv:2410.16488 (2024). <<https://ui.adsabs.harvard.edu/abs/2024arXiv241016488G>>.
- 25 Chung, Y. C., Heiblum, M. & Umansky, V. Scattering of bunched fractionally charged quasiparticles. *Physical Review Letters* **91**, 216804 (2003).
<https://doi.org/10.1103/PhysRevLett.91.216804>
- 26 Bid, A., Ofek, N., Heiblum, M., Umansky, V. & Mahalu, D. Shot noise and charge at the $2/3$ composite fractional quantum Hall state. *Phys Rev Lett* **103**, 236802 (2009).
<https://doi.org/10.1103/PhysRevLett.103.236802>
- 27 Bhattacharyya, R., Banerjee, M., Heiblum, M., Mahalu, D. & Umansky, V. Melting of interference in the fractional quantum Hall effect: Appearance of neutral modes. *Physical Review Letters* **122**, 246801 (2019).
<https://doi.org/10.1103/PhysRevLett.122.246801>
- 28 Biswas, S. *et al.* Shot noise does not always provide the quasiparticle charge. *Nature Physics* (2022). <https://doi.org/10.1038/s41567-022-01758-x>
- 29 Deviatov, E. V., Egorov, S. V., Biasiol, G. & Sorba, L. Quantum Hall Mach-Zehnder interferometer at fractional filling factors. *Europhysics Letters* **100**, 67009 (2012).
<https://doi.org/10.1209/0295-5075/100/67009>
- 30 Batra, N., Wei, Z., Vishveshwara, S. & Feldman, D. E. Anyonic Mach-Zehnder interferometer on a single edge of a two-dimensional electron gas. *Physical Review B* **108**, L241302 (2023). <https://doi.org/10.1103/PhysRevB.108.L241302>
- 31 Moore, G. & Read, N. Nonabelions in the fractional quantum Hall effect. *Nuclear Physics B* **360**, 362-396 (1991). [https://doi.org/10.1016/0550-3213\(91\)90407-O](https://doi.org/10.1016/0550-3213(91)90407-O)

Acknowledgments

M.H. thanks Yuval Ronen for the fruitful discussions.

D.F.M. acknowledges many illuminating conversations on quantum Hall interferometry with Yuval Ronen.

B.G thanks Arup Kumar Paul for the helpful comments that improved our device.

M.L. thanks the Ariane de Rothschild Women Doctoral Program for their support

D.F.M. acknowledges the support of the Israel Science Foundation (ISF) under Grant No. 2572/21 and by the Deutsche Forschungsgemeinschaft (DFG) within the CRC network TR 183 (project Grant No. 277101999).

M.H. acknowledges the support of the European Research Council under the European Union's Horizon 2020 research and innovation program. (Grant Agreement No. 833078) and by the Israel Science Foundation (ISF) under Grant No. 1510/22.

Supplementary Material

S1. Sample fabrication process

The MESA of the device, with dimensions $250 \times 650 \text{ } \mu\text{m}^2$, was prepared in GaAs/AlGaAs heterostructure by wet etching in $\text{H}_2\text{O}_2: \text{H}_3\text{PO}_4: \text{H}_2\text{O} = 1:1:50$ for 100 seconds. The 2DEG was located 170 nm below the surface. Ohmic contacts were deposited at the edge of the MESA and within the MESA area (for testing the interface modes). The sequence of the evaporation by order was: Ni (15 nm), Au (260 nm), Ge (130 nm), Ni (87.5 nm), Au (15 nm). Contacts were annealed at 440°C for 80 seconds. The sample was covered by 30 nm of an insulating HfO_2 followed by evaporation of large metal gates, Ti (5 nm) and Au (15 nm). The latter separated the device area into three regions with fillings: ν_a , ν_b , ν_d . In the following step, the MESA was covered by 25 nm of HfO_2 layer, followed by a deposition of quantum point contacts (QPCs), a modulation gate (MG), and a small top gate (TG) in the middle of the bulk, with diameter $0.5 \text{ } \mu\text{m}$ and or $0.35 \text{ } \mu\text{m}$. In the final step, ohmic contacts, large metallic gates, the QPCs, and the modulation gate (MG) were connected to large pads via thick gold lines. The TG was connected by an *air bridge* and gold lines that passed over the HfO_2 -coated metallic gates.

S2. Interfacing hole-conjugate states

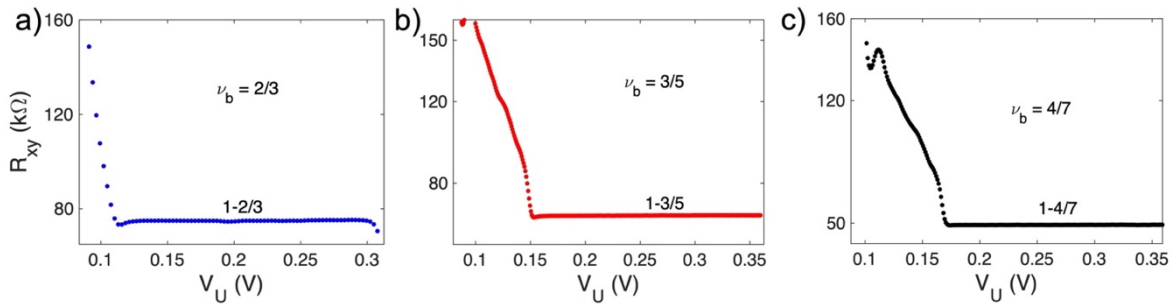


Figure S2. Interfacing hole-conjugate states. Two-terminal resistance measurements of the interface between ν_b and ν_a . The bulk filling factor is fixed at $\nu_b = 2/3$ (a), $3/5$ (b), and $4/7$ (c), while the accumulation gate is swept on the conductance plateau of $\nu_a = 1$, with a positive bias. At $\nu_b = 2/3$ and $\nu_a = 1$, the 2DEG density underneath the gate increases by $\sim 50\%$. Once charge equilibration is achieved, all interface modes move in the downstream direction.

S3. Dependence of flux periodicity on the interface modes

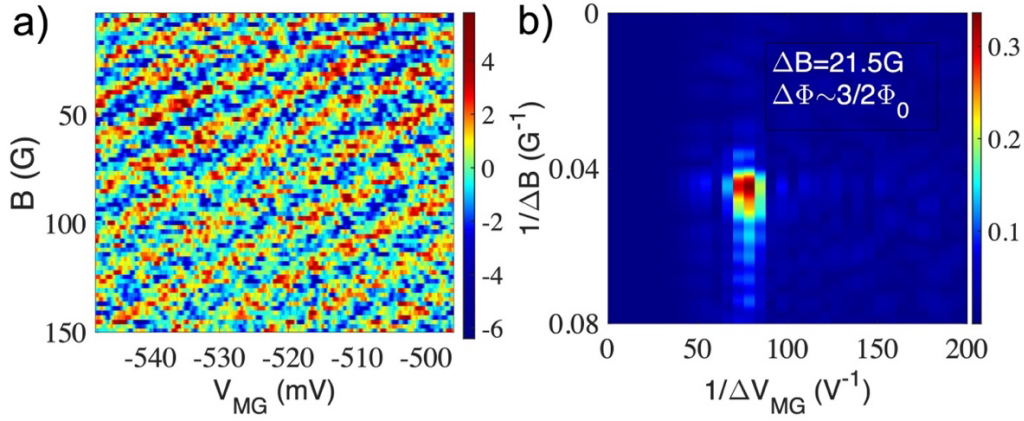


Figure S3. Aharonov-Bohm interference configuration $\nu_a=4/3$, $\nu_b=2/3$, $\nu_d=0$. (a) Conductance oscillations for $\nu_b=2/3$ in the B - V_{MG} plane, with 2DEG density underneath the accumulation gate is increased by $\sim 100\%$. The top gate in the bulk is not charged ($V_{TG}=0$ V). (b) The 2D FFT of the pajama plot shows a single peak with the periodicity $\Delta B=21.5$ G, $\Delta V_{MG}=12.7$ mV. The flux periodicity is $\Delta \Phi \approx (3/2)\Phi_0$, for an AB area of $\sim 3\mu\text{m}^2$. Similar results were observed in the fillings combination '1-2/3-0' (see main text) and '1-2/3-1/3', suggesting that the bulk filling solely determines the flux periodicity. Although the configuration of the upstream neutral mode is different in the configuration 4/3-2/3-0 (downstream neutral at '4/3-2/3' and upstream neutral at '2/3-0') and in 1-2/3-0 (one upstream neutral mode at the '2/3-0' interface) and 1-2/3-1/3 (two upstream neutral at '2/3-1/3' interface), all suggesting that the fractional flux periodicity is not affected by the nature of the edge modes.

S4. The effect of positive top gate potential on the bunched anyons

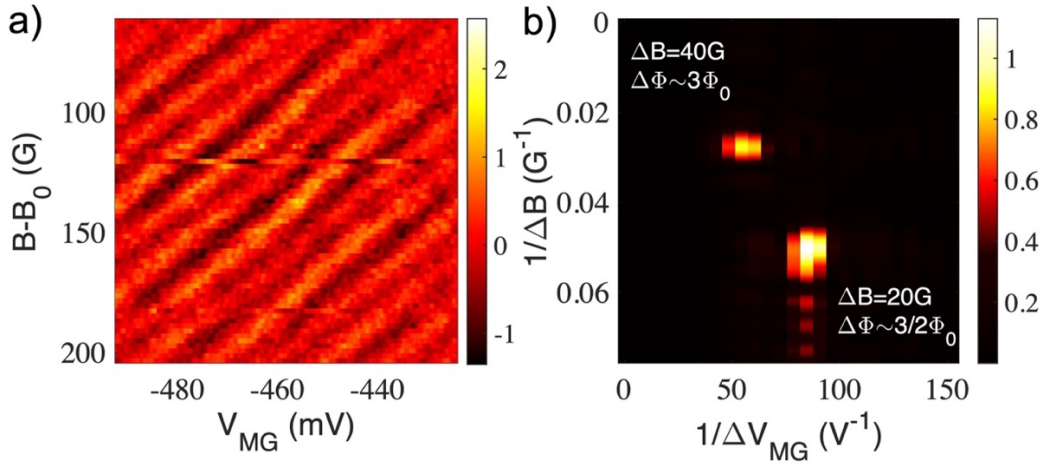


Figure S4. Dissociation of bunched anyons via charging the TG: (a) AB pajama with $\nu_b=2/3$, and filling factors configuration: '1-2/3-0'. The QPCs are biased for transmission of 80% and top gate voltage is $V_{TG}=+0.03$ V. (b) 2D FFT with two distinct peaks: The most prominent peak with flux periodicity $\Delta \Phi \sim (3/2)\Phi_0$ corresponds to the interference of a 'bunched' QP with charge $2e/3$. The weaker peak with flux periodicity $\Delta \Phi \sim 3\Phi_0$ corresponds to the interference of elementary QPs with a charge $e/3$, suggesting partial dissociation of the bunched QPs. Note that the modulation gate voltage periodicity (ΔV_{MG}) is almost twice as large in the dissociated condition. For a negative TG potential, see the main text.

S5. Analysis of the deconvoluted peaks using the Gaussian filtering method

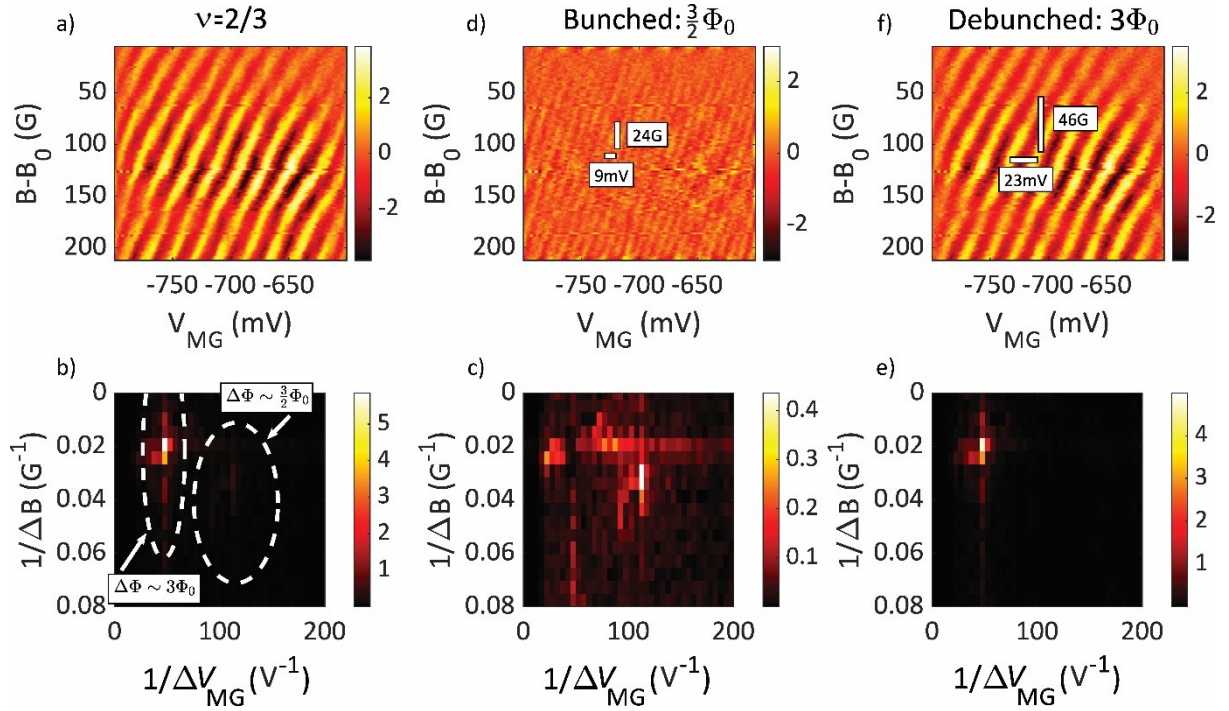


Figure S5a. Separate views of flux periodicities at filling $\nu=2/3$ with charged top gate. (a) A strong peak at $\Delta\Phi=3\Phi_0$ (dissociated QPs) and a residual peak at $\Delta\Phi\cong(3/2)\Phi_0$ (bunched QPs) (b) Two corresponding peaks in the FFT. The dotted ovals indicate the radius of the Gaussian filtering applied later. (c) Removing the dissociated FFT peak at $3\Phi_0$ by Gaussian filtering and leaving the weaker peak of the bunched QPs. (d) Returning to *real space* pajama of the bunched QPs, with periodicity $\Delta\Phi\cong(3/2)\Phi_0$. (e) Filtering the residual bunched FFT peak. (f) Returning to *real space* pajama of the dissociated ('unbunched') elementary QPs, $\Delta\Phi\cong3\Phi_0$.

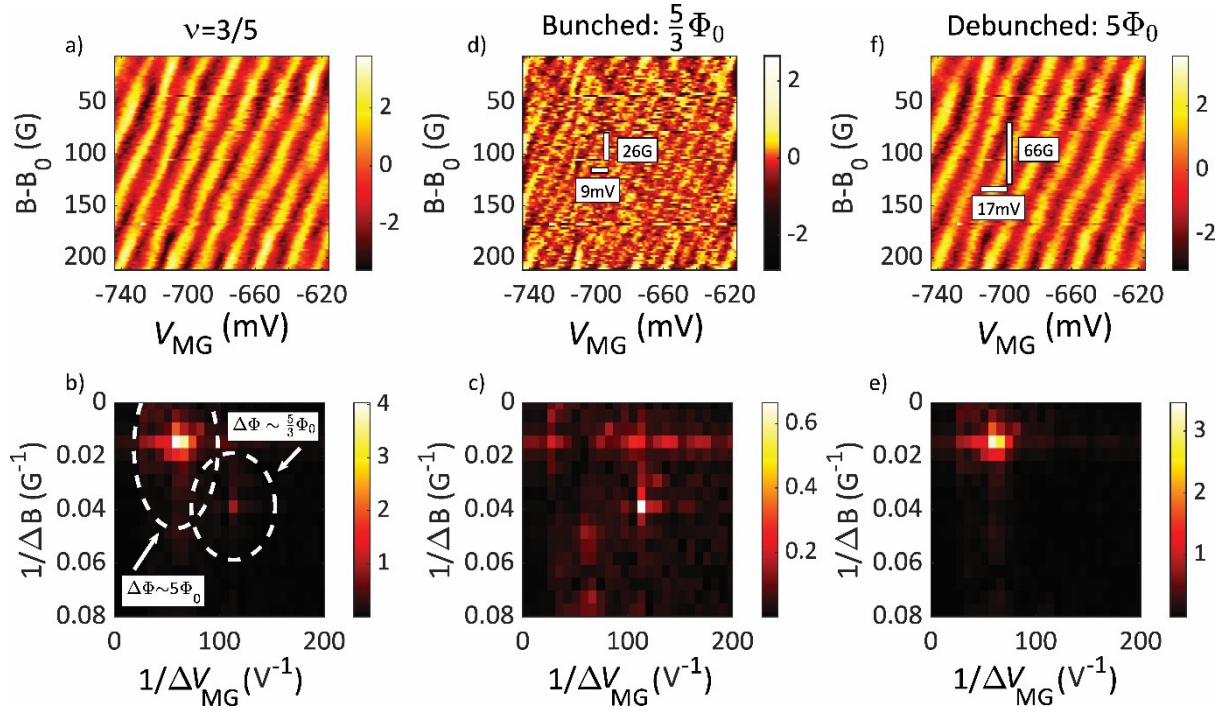


Figure S5b. Separate views of flux periodicities at filling $\nu=3/5$ with charged top gate. (a) A strong peak at $\Delta\Phi \cong 5\Phi_0$ (dissociated QPs) and a residual peak at $\Delta\Phi \cong (5/3)\Phi_0$ (bunched QPs) (b) Two corresponding peaks in the FFT. The dotted ovals indicate the radius of the Gaussian filtering applied later. (c) Removing the dissociated FFT peak at $5\Phi_0$ by Gaussian filtering and leaving the weaker peak of the bunched QPs. (d) Returning to *real space* pajama of the bunched QPs, with periodicity $\Delta\Phi \cong (5/3)\Phi_0$. (e) Filtering the residual bunched FFT peak. (f) Returning to *real space* pajama of the dissociated elementary QPs, $\Delta\Phi \cong 5\Phi_0$.

S6. The effect of temperature on the interference

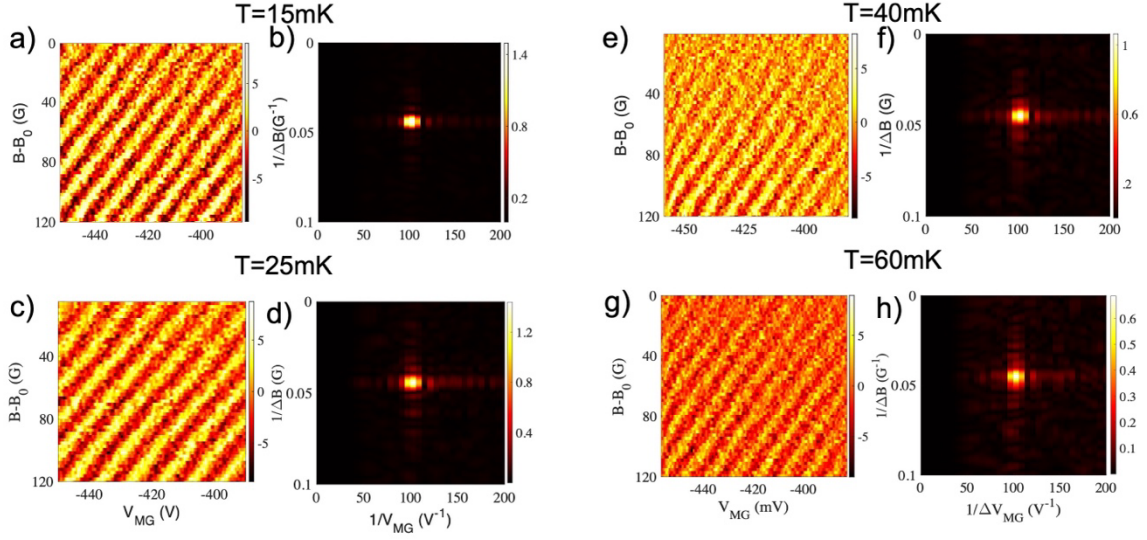


Figure S6. The effect of temperature increase on the bunching of QPs at $\nu_b=3/5$. AB interference at an elevated electron temperature in the range 15-100mK with QPCs transmission of: $T_1 = T_2=0.8$. In the range 15-60mK the visibility remains nearly constant ($\sim 1\%$) while the 2D-FFT plots remain with a single prominent peak of bunched QPs, $\Delta\Phi \sim (5/3)\Phi_0$. Above 60mK the visibility drops abruptly. Similar measurements were also performed at $\nu=2/3$ (not shown in the figure), showing qualitatively similar results. The decrease of the visibility with increased temperature prevents an observation of the dissociation.

S7. Bunching and dissociation of the interference in the device with smaller top-gate

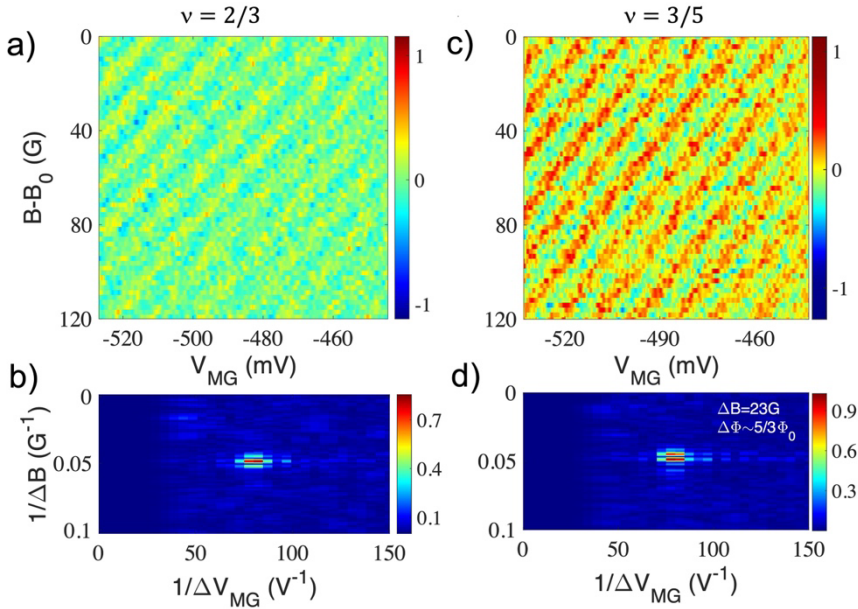


Figure S7a. Aharonov Bohm interference at $\nu_b=2/3$ and $3/5$ – Bunching. The OMZI was fabricated on the same wafer. The interferometer area ($\sim 3\mu\text{m}^2$) and path length ($\sim 3\mu\text{m}$) similar to the main device described in the text. However, the QPCs are relatively open, and the top-gate area is half of the original one. Here, $V_{\text{TG}}=0\text{V}$, with interference of bunched QPs in $\nu_b=2/3$ (a,b) and $\nu_b=3/5$ (c,d) . The B - V_{MG} interference similar to the main device.

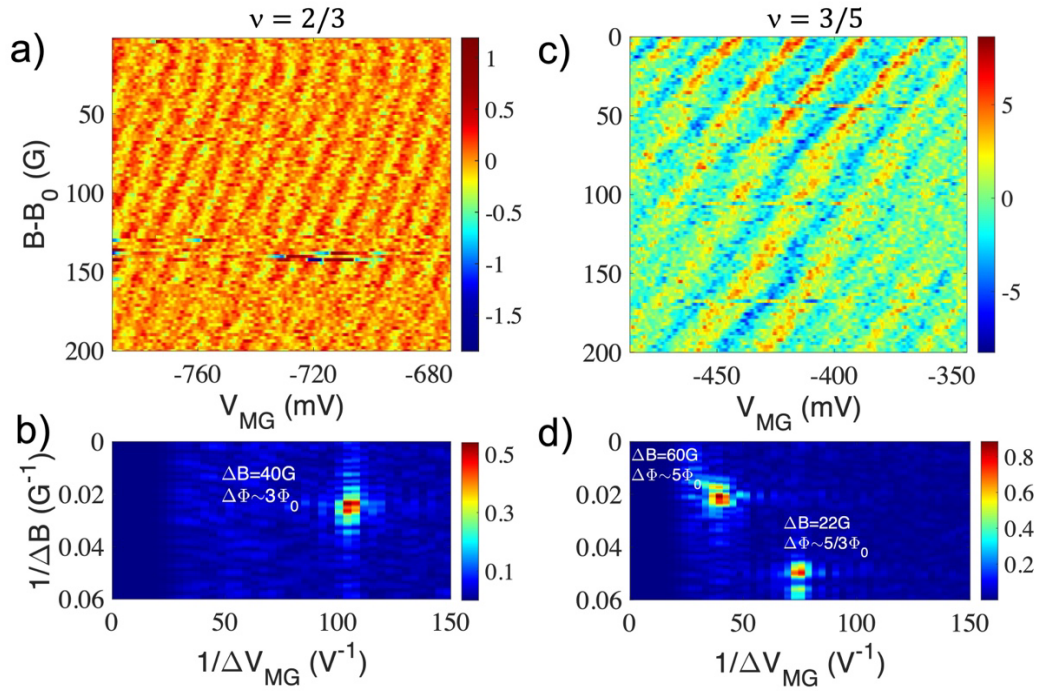


Figure S7b. Aharonov Bohm interference at $\nu_b=2/3$ and $3/5$ – Dissociation. Aharonov Bohm oscillation at $\nu_b = 2/3$ and $3/5$ for the filling factor configurations **(a)** ‘1-2/3-0’ **(c)** ‘1-3/5-0’. For this measurement, the top-gate was charged at $V_{TG}=+(0.03-0.05)V$ and the QPCs were tuned to transmission of 90%. 2D FFT shows magnetic flux periodicity corresponding to $\Delta\Phi \cong 3\Phi_0$ for $\nu_b = 2/3$ in **(b)** and $\Delta\Phi \cong 5\Phi_0$ for $\nu_b = 3/5$ in **(d)** suggesting a dissociation of the QPs. Additionally, a small residual harmonic, $\Delta\Phi \cong (5/3)\Phi_0$, indicative of bunched QPs, is present at $\nu_b=3/5$. **(d)**. However, this harmonic is absent for $\nu_b = 2/3$ **(b)** (likely due to its low visibility).